

# Spacetime structures of continuous time quantum walks

Oliver Mülken and Alexander Blumen

*Theoretische Polymerphysik, Universität Freiburg, Hermann-Herder-Straße 3, 79104 Freiburg i.Br., Germany*

(Dated: January 19, 2022)

The propagation by continuous time quantum walks (CTQWs) on one-dimensional lattices shows structures in the transition probabilities between different sites reminiscent of quantum carpets. For a system with periodic boundary conditions, we calculate the transition probabilities for a CTQW by diagonalizing the transfer matrix and by a Bloch function ansatz. Remarkably, the results obtained for the Bloch function ansatz can be related to results from (discrete) generalized coined quantum walks. Furthermore, we show that here the first revival time turns out to be larger than for quantum carpets.

PACS numbers: 05.60.Gg, 05.40.-a, 03.67.-a

Simple theoretical models have always been very useful for our understanding of physics. In quantum mechanics, next to the harmonic oscillator, the particle in a box provides much insight into the quantum world (e.g. [1]). Recently, the problem of a quantum mechanical particle initially characterized by a gaussian wave packet and moving in an infinite box has been reexamined [2, 3, 4]. Surprisingly, this simple system shows complex but regular spacetime probability structures which are now called quantum carpets.

In solid state physics and quantum information theory, one of the most simple systems is associated with a particle moving in a regular periodic potential. This can be, for instance, either an electron moving through a crystal [5, 6] or a qubit on an optical lattice or in an optical cavity [7, 8, 9]. For the electron moving through a crystal, the band structure and eigenfunctions are well known. In principle, the same holds for the qubit. However, in quantum information theory, the qubit on a lattice or, more general, on a graph is used to define the quantum analog of a random walk. As classically, there is a discrete [10] and a continuous-time [11] version. Unlike in classical physics, these two are not translatable into each other.

Here we focus on continuous-time (quantum) random walks. Consider a walk on a graph which is a collection of connected nodes. Lattices are very simple graphs where the nodes are connected in a very regular manner. To every graph there exists a corresponding adjacency or connectivity matrix  $\mathbf{A} = (A_{ij})$ , which is a discrete version of the Laplace operator. The non-diagonal elements  $A_{ij}$  equal  $-1$  if nodes  $i$  and  $j$  are connected by a bond and  $0$  otherwise. The diagonal elements  $A_{ii}$  equal the number of bonds which exit from node  $i$ , i.e.,  $A_{ii}$  equals the functionality  $f_i$  of the node  $i$ .

Classically, a continuous-time random walk (CTRW) is governed by the master equation [12, 13]

$$\frac{d}{dt}p_{jk}(t) = \sum_l T_{jl} p_{lk}(t), \quad (1)$$

where  $p_{jk}(t)$  is the conditional probability to find the CTRW at time  $t$  at node  $j$  when starting at node  $k$ . The transfer matrix of the walk,  $\mathbf{T} = (T_{jk})$ , is related to the adjacency matrix by  $\mathbf{T} = -\gamma\mathbf{A}$ , where we assume the transmission rate  $\gamma$  of all bonds to be equal for simplicity. Formally, this approach can be generalized to continuous models like the Lorentz gas [14].

The formal solution of Eq.(1) is

$$p_{jk}(t) = \langle j | e^{\mathbf{T}t} | k \rangle. \quad (2)$$

The quantum-mechanical extension of a CTRW is called continuous-time quantum walk (CTQW). These are obtained by identifying the Hamiltonian of the system with the (classical) transfer operator,  $\mathbf{H} = -\mathbf{T}$  [11, 15, 16]. Then the basis vectors  $|k\rangle$  associated with the nodes  $k$  of the graph span the whole accessible Hilbert space. In this basis the Schrödinger equation (SE) reads

$$i\frac{d}{dt}|k\rangle = \mathbf{H}|k\rangle, \quad (3)$$

where we have set  $m \equiv 1$  and  $\hbar \equiv 1$ . The time evolution of a state  $|k\rangle$  starting at time  $t_0$  is given by  $|k(t)\rangle = \mathbf{U}(t, t_0)|k\rangle$ , where  $\mathbf{U}(t, t_0) = \exp(-i\mathbf{H}(t - t_0))$  is the quantum mechanical time evolution operator. Now the transition amplitude  $\alpha_{jk}(t)$  from state  $|k\rangle$  at time  $0$  to state  $|j\rangle$  at time  $t$  reads

$$\alpha_{jk}(t) = \langle j | e^{-i\mathbf{H}t} | k \rangle. \quad (4)$$

Following from Eq.(3) the  $\alpha_{jk}(t)$  obey

$$i\frac{d}{dt}\alpha_{jk}(t) = \sum_l H_{jl}\alpha_{lk}(t). \quad (5)$$

The main difference between Eq.(2) and Eq.(4) is that classically  $\sum_j p_{jk}(t) = 1$ , whereas quantum mechanically  $\sum_j |\alpha_{jk}(t)|^2 = 1$  holds.

In principle, for the full solution of Eqs.(1) and (5) all the eigenvalues and all the eigenvectors of  $\mathbf{T} = -\mathbf{H}$  (or, equivalently, of  $\mathbf{A}$ ) are needed. Let  $\lambda_n$  denote the  $n$ th eigenvalue of  $\mathbf{A}$  and  $\mathbf{\Lambda}$  the corresponding eigenvalue matrix. Furthermore, let  $\mathbf{Q}$  denote the matrix constructed from the orthonormalized eigenvectors of  $\mathbf{A}$ , so that  $\mathbf{A} = \mathbf{Q}\mathbf{\Lambda}\mathbf{Q}^{-1}$ . Now the classical probability is given by

$$p_{jk}(t) = \langle j | \mathbf{Q} e^{-t\gamma\mathbf{\Lambda}} \mathbf{Q}^{-1} | k \rangle, \quad (6)$$

whereas the quantum mechanical transition probability is

$$\pi_{jk}(t) \equiv |\alpha_{jk}(t)|^2 = |\langle j | \mathbf{Q} e^{-it\gamma\mathbf{\Lambda}} \mathbf{Q}^{-1} | k \rangle|^2. \quad (7)$$

The unitary time evolution prevents that  $\pi_{jk}(t)$  has a definite limit for  $t \rightarrow \infty$ . In order to compare the classical long

time probability with the quantum mechanical one, one usually uses the limiting probability distribution [17]

$$\chi_{kj} \equiv \lim_{T \rightarrow \infty} \frac{1}{T} \int_0^T dt \pi_{jk}(t). \quad (8)$$

In the subsequent calculation we restrict ourselves to CTQWs on regular one-dimensional (1d) lattices. Then the adjacency matrix  $\mathbf{A}$  takes on a very simple form. For a 1d lattice with periodic boundary conditions, i.e. a circle, every node has exactly two neighbors. Thus, for a lattice of length  $N$ , with the boundary condition that node  $N+1$  is equivalent to node 1, we have

$$\mathbf{A} = (A_{ij}) = \begin{cases} 2 & i = j \\ -1 & i = j \pm 1 \\ 0 & \text{else.} \end{cases} \quad (9)$$

For a lattice with reflecting boundary conditions the adjacency matrix  $\mathbf{A}$  is analogous to Eq.(9), except that  $A_{11} = A_{NN} = 1$  and  $A_{1N} = A_{N1} = 0$  because the end nodes have only one neighbor. Solving the eigenvalue problem for  $\mathbf{A}$ , which is a real and symmetric matrix is a well-known problem, also of much interest in polymer physics [18, 19]. A different ansatz describing the dynamics of a quantum particle in 1d was given by Wójcik and Dorfman who employ a quantum multibaker map [20].

The structure of  $\mathbf{H} = \gamma \mathbf{A}$  suggests an analytic treatment. For a 1d lattice with periodic boundary conditions and  $\gamma = 1$  the Hamiltonian acting on a state  $|j\rangle$  is given by

$$\mathbf{H}|j\rangle = 2|j\rangle - |j-1\rangle - |j+1\rangle, \quad (10)$$

which is the discrete version of the Laplacian  $-\Delta = -\nabla^2$ . Eq.(10) is the discrete version of the Hamiltonian for a free particle moving on a lattice. It is well known in solid state physics that the solutions of the SE for a particle moving freely in a regular potential are Bloch functions [5, 6]. Thus, the time independent SE is given by

$$\mathbf{H}|\Phi_\theta\rangle = E_\theta|\Phi_\theta\rangle, \quad (11)$$

where the eigenstates  $|\Phi_\theta\rangle$  are Bloch states and can be written as a linear combination of states  $|j\rangle$  localized at nodes  $j$ ,

$$|\Phi_\theta\rangle = \frac{1}{\sqrt{N}} \sum_{j=1}^N e^{-i\theta j} |j\rangle. \quad (12)$$

The projection on the state  $|j\rangle$  then reads  $\Phi_\theta(j) \equiv \langle j|\Phi_\theta\rangle = e^{-i\theta j}/\sqrt{N}$ , which is nothing but the Bloch relation  $\Phi_\theta(j+1) = e^{-i\theta} \Phi_\theta(j)$  [5, 6]. Now the energy is obtained from Eqs.(11) and (12) as

$$E_\theta = 2 - 2 \cos \theta. \quad (13)$$

For small  $\theta$  the energy is given by  $E_\theta \approx \theta^2$  which resembles the energy spectrum of a free particle.

With this ansatz we calculate the transition amplitudes  $\alpha_{kj}(t)$ . The state  $|j\rangle$  is localized at node  $j$  and may be described by a Wannier function [5, 6], i.e. by inverting Eq.(12),

$$|j\rangle = \frac{1}{\sqrt{N}} \sum_{\theta} e^{i\theta j} |\Phi_\theta\rangle. \quad (14)$$

Since the states  $|j\rangle$  span the whole accessible Hilbert space, we have  $\langle k|j\rangle = \delta_{kj}$  and therefore via Eq.(12) also  $\langle \Phi_{\theta'}|\Phi_\theta\rangle = \delta_{\theta'\theta}$ .

Then the transition amplitude reads

$$\begin{aligned} \alpha_{kj}(t) &= \frac{1}{N} \sum_{\theta, \theta'} \langle \Phi_{\theta'}| e^{-i\theta k} e^{-i\mathbf{H}t} e^{i\theta' j} |\Phi_\theta\rangle \\ &= \frac{1}{N} \sum_{\theta} e^{-iE_\theta t} e^{-i\theta(k-j)}. \end{aligned} \quad (15)$$

The periodic boundary condition for a 1d lattice of size  $N$  requires  $\Phi_\theta(N+1) = \Phi_\theta(1)$ , thus  $\theta = 2n\pi/N$  with  $n \in [0, N]$ . Now Eq.(15) is given by

$$\alpha_{kj}(t) = \frac{e^{-i2t}}{N} \sum_n e^{i2t \cos(2n\pi/N)} e^{-i2\pi n(k-j)/N}. \quad (16)$$

For small  $\theta$ , this result is directly related to the results obtained for a quantum particle in a box [2, 3, 4], because then we have  $E_n \sim n^2$ .

In the limit  $N \rightarrow \infty$ , Eq.(16) translates to

$$\begin{aligned} \lim_{N \rightarrow \infty} \alpha_{kj}(t) &= \frac{e^{-i2t}}{2\pi} \int_{-\pi}^{\pi} d\theta e^{-i\theta(k-j)} e^{i2t \cos \theta} \\ &= i^{k-j} e^{-i2t} J_{k-j}(2t), \end{aligned} \quad (17)$$

where  $J_k(x)$  is the Bessel function of the first kind [21]. The same result has also been obtained with a functional integral ansatz [22]. From Eq.(17) we also see that the first maxima of the transition probabilities are related to the maxima of the Bessel function, since we have  $\lim_{N \rightarrow \infty} \pi_{kj}(t) = [J_{k-j}(2t)]^2$ . However, for an infinite lattice there is no interference due to either backscattering at reflecting boundaries or transmission by periodic boundaries.

For higher dimensional lattices the calculation is analogous. We note that the assumption of periodic boundary conditions is strictly valid only in the limit of very large lattice sizes where the exact form of the boundary does not matter [5, 6].

Very recently it has been found by Wójcik *et al.*, [23], that the return probability for a 1d generalized coined quantum walk (GCQW), which is a variant of a discrete quantum walk, has the functional form  $p_{kk}(t\tau) = [J_0(2t\sqrt{D})]^2$ , where  $\tau$  and  $D$  are variables specified in [23], which indeed is of the same form as the return probability calculated from Eq.(17). We interpret this as an indication that CTQWs and GCQWs, although not directly translatable into each other, can lead to similar results. However, in [23] the return probability is calculated for a particle on a very large circle such that interference effects are not seen on the short time scales considered

there. By looking ahead at Fig. 1, we see that, indeed, on short time scales this is also approximately true in our case of the CTQW on the finite lattice. Nevertheless, without going into further detail at this point, we note this remarkable similarity between CTQWs and GCQWs.

For a CTQW on a 1d circular lattice we calculate the quantum mechanical transition probabilities  $\pi_{jk}(t)$ . Figure 1(a) shows the return probability  $\pi_{kk}(t)$  for a CTQW on a circle of 21 nodes first evaluated in a straightforward way by diagonalizing the matrix  $\mathbf{A}$  numerically, then by using the Bloch function ansatz described above. Both results coincide. For comparison we also have computed the return probability for the infinitely extended system, see Eq.(17). On small time scales all the results coincide. At later times waves propagating on the finite lattice start to interfere; then the results diverge and for a finite lattice one observes an increase in the probability of being at the starting node. This happens around the time  $t \approx N/2$ .

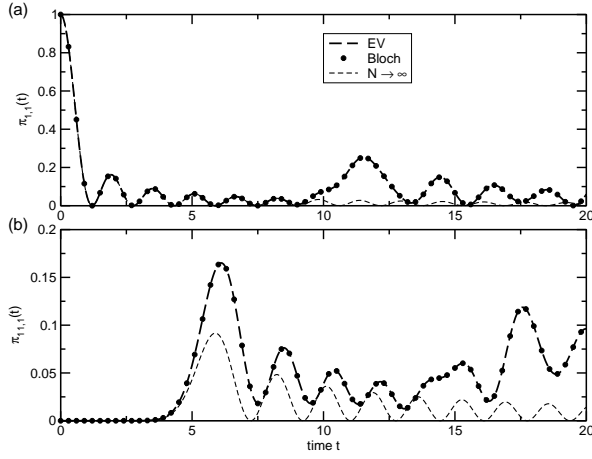


FIG. 1: Plot for a CTQW on a circle of length  $N = 21$  of (a) the return probability and (b) the transition probability to go in time  $t$  from the starting node to the opposite node on the circle. Time is given in units of the inverse transmission rate  $\gamma^{-1}$ . The results using Eq.(7), long dashed line, and Eq.(16), full circles, are compared to the limit  $N \rightarrow \infty$ , short dashed line.

In Fig. 1(b) the probability to go from a starting node to the farthest node on the circle, here to go from node 1 to node 11 (or 12), is plotted. Again the calculations by the eigenvalue method and by the Bloch function ansatz are indistinguishable. As before, also the probabilities for the infinite and for the finite systems differ. The difference is more pronounced because in time  $t \approx N/4$  counterpropagating waves from the starting node interfere at the opposite node.

The probabilities to go from a starting node to all other nodes in time  $t$  on a circle of length  $N = 21$  is plotted in Fig. 2(left). (For a CTQW on a circle the starting node is arbitrary.) For small times, when there is no interference, the waves propagate freely. After a time  $t \approx N/4$  the waves interfere but the pattern remains quite regular. The same holds for  $N = 20$ , but the structures are more regular, see Fig. 2(right). This is due to the fact that the number of steps to go from one node to another is even or odd in both directions for the even-

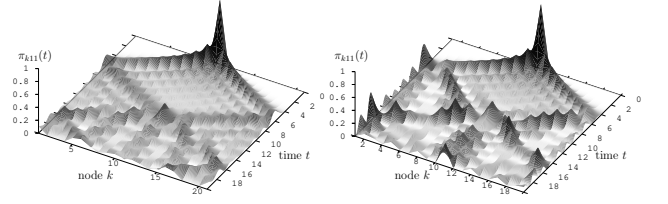


FIG. 2: Plot of the probability for a CTQW on a circle of length  $N = 21$  (left) and  $N = 20$  (right) over time  $t$  to go from a starting node to all other nodes. See Fig.1 for units.

numbered circle, where it is even in one and odd in the other direction for the odd-numbered circle.

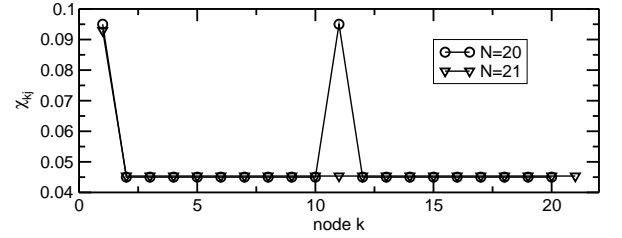


FIG. 3: Limiting probability distribution  $\chi_{kj}$  for a CTQW on a circle of length  $N = 20$  (circles) and  $N = 21$  (triangles).

Figure 3 supports this. The limiting distribution  $\chi_{kj}$  has two maxima for  $N = 20$ , one at the starting node 1 and one at the opposite node 11, reflecting the higher symmetry of the lattice. Whereas there is only one maximum for  $N = 21$  at the starting node 1.

At this point it is instructive to look at very small circles of  $N = 3$  and 4 nodes where the analytic results are still handy. With Eq.(16) we find for the transition probabilities for  $N = 3$ ,

$$\pi_{kj}(t) = \begin{cases} \frac{5}{9} + \frac{16}{9} \cos^3 t - \frac{4}{3} \cos t & k = j \\ \frac{2}{9} - \frac{8}{9} \cos^3 t - \frac{2}{3} \cos t & k \neq j. \end{cases} \quad (18)$$

For  $N = 4$  we have

$$\pi_{kj}(t) = \begin{cases} \cos^4 t & k = j \\ \sin^4 t & k = 2j \\ \sin^2 t \cos^2 t & \text{else,} \end{cases} \quad (19)$$

where  $\pi_{jj}(t)$  and  $\pi_{j,2j}(t)$  are only shifted by a phase factor of  $\pi/2$  but equal in magnitude. The limiting probability distributions are for  $N = 3$ ,  $\chi_{11} = 5/9$  and  $\chi_{12} = \chi_{13} = 2/9$  and for  $N = 4$ ,  $\chi_{11} = \chi_{13} = 3/8$  and  $\chi_{12} = \chi_{14} = 1/8$ , and thus support the findings for bigger lattices, e.g. Fig. 3.

The occurrence of the regular structures is reminiscent of the so-called quantum carpets [2, 3, 4]. These were found in the interference pattern of a quantum particle, initially prepared as a gaussian wave packet, moving in a 1d box. The spreading and self-interference due to reflection of the wave packet at the walls lead to patterns in the spacetime probability distribution. Furthermore, after some time, the so-called revival time, the whole initial wavefunction gets reconstructed. For a particle in a box, these quantum revivals are

(almost) perfect and the revival time  $T$  follows from the energy  $E_n = (n\pi\hbar/L)^2/2m = n^2 2\pi\hbar/T$ , where  $L$  is the width of the box [3].

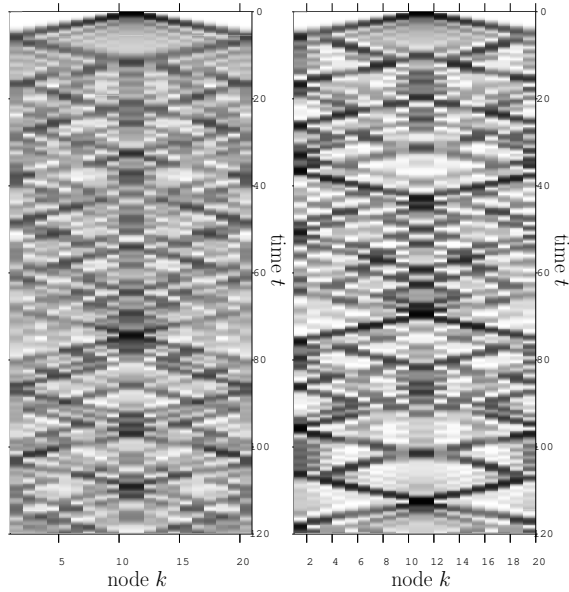


FIG. 4: Contour plot of the probability for a CTQW on a circle of length  $N = 21$  (left) and  $N = 20$  (right) over longer times  $t$  than in Fig. 2. Dark regions denote high probabilities. See Fig.1 for units.

For very long times, Fig. 4 shows a contour plot of the probability for a CTQW on a circle of length  $N = 21$  (left) and  $N = 20$  (right). There is obvious structure in the interference pattern. Furthermore, there are areas on this quantum carpet where there is a very high probability, visualized by dark regions, to find the CTQW at its starting point. Thus, quantum revivals also occur for the discrete lattice. However, these are not perfect.

The revival time  $\tau$  is given by  $\alpha_{kj}(\tau) = \alpha_{kj}(0)$ . Since the transition amplitudes are given as a sum over all modes  $n$ , see Eq.(16), we cannot give a universal revival time which is

independent of  $n$ . Nevertheless, from Eq.(16) we get for each mode  $n$  its revival time

$$\tau_n = \frac{r\pi}{1 - \cos(2n\pi/N)} = \frac{r\pi}{2}[1 + \cot^2(n\pi/N)], \quad (20)$$

where  $r \in \mathbb{N}$  (without any loss of generality we set  $r = 1$ ). From Eq.(20) we find that  $\tau_n > \tau_{n+1}$  for  $n \in ]0, N/2]$  and  $\tau_n < \tau_{n+1}$  for  $n \in ]N/2, N]$ . For certain values of  $n$ ,  $\tau_n$  will be of order unity, e.g. for  $n = N/2$  we get  $\tau_n = \pi/2$ . However, for  $n \ll N$ , Eq.(20) yields  $\tau_n = N^2/2\pi n^2 \equiv \tau_0/n^2$ , which is analogous to the particle in the box and where  $\tau_0$  is a universal revival time. Thus, the revival times  $\tau_n$  have large variations in value. To make a sensible statement about at least the first revival time, we need to compare it to the actual time needed by the CTQW for travelling through the lattice. As mentioned earlier, interference effects in the return probability  $\pi_{1,1}(t)$  are seen after a time  $t \approx N/2$ . The first revival time has to be larger than this, because there cannot be any revival unless the wave reaches its starting node again. Our calculations suggest that the first revival time will be of order  $\tau_0$ . From Fig. 4 we see that the first (incomplete) revival occurs for  $N = 20$  at  $t \approx 70 > 20^2/2\pi$  and for  $N = 21$  at  $t \approx 75 > 21^2/2\pi$ .

In conclusion we have shown that CTQWs on regular 1d lattices show regular structures in their spacetime transition probabilities. By employing the Bloch function ansatz we calculated quantum mechanical transition probabilities (as a function of time  $t$ ) between the different nodes of the lattice. These results are practically indistinguishable from the ones obtained by diagonalizing the transfer matrix. We note that the results obtained via the Bloch function ansatz can be related to recent results for GCQWs. The spacetime structures are reminiscent of quantum carpets, but have their first revival at later times than what is found for quantum carpets.

Support from the Deutsche Forschungsgemeinschaft (DFG) and the Fonds der Chemischen Industrie is gratefully acknowledged.

- 
- [1] J. Sakurai, *Modern Quantum Mechanics* (Addison-Wesley Publishing Company, 1994), 2nd ed.
  - [2] W. Kinzel, Phys. Bl. **51**, 1190 (1995).
  - [3] F. Grossmann, J.-M. Rost, and W. P. Schleich, J. Phys. A **30**, L277 (1997).
  - [4] M. V. Berry, J. Phys. A **29**, 6617 (1996).
  - [5] J. M. Ziman, *Principles of the Theory of Solids* (Cambridge University Press, 1972).
  - [6] C. Kittel, *Introduction to Solid State Physics* (John Wiley & Sons, 1986).
  - [7] J. Kempe, Contemporary Physics **44**, 307 (2003).
  - [8] P. L. Knight, E. Roldán, and J. E. Sipe, Opt. Comm. **227**, 147 (2003).
  - [9] W. Dür, R. Raussendorf, V. M. Kendon, and H.-J. Briegel, Phys. Rev. A **66**, 052319 (2002).
  - [10] Y. Aharonov, L. Davidovich, and N. Zagury, Phys. Rev. A **48**, 1687 (1993).
  - [11] E. Farhi and S. Gutmann, Phys. Rev. A **58**, 915 (1998).
  - [12] G. H. Weiss, *Aspects and Applications of the Random Walk* (North-Holland, 1994).
  - [13] N. van Kampen, *Stochastic Processes in Physics and Chemistry* (North-Holland, 1990).
  - [14] O. Mülken and H. van Beijeren, Phys. Rev. E **69**, 046203 (2004).
  - [15] O. Mülken and A. Blumen, Phys. Rev. E **71**, 016101 (2005).
  - [16] A. M. Childs, E. Farhi, and S. Gutmann, Quantum Information Processing **1**, 35 (2002).
  - [17] D. Aharonov, A. Ambainis, J. Kempe, and U. Vazirani, in *Proceedings of ACM Symposium on Theory of Computation (STOC'01)* (2001), p. 50.
  - [18] A. Blumen, A. Jurjiu, T. Koslowski, and C. von Ferber, Phys. Rev. E **67**, 061103 (2003).
  - [19] A. Blumen, C. von Ferber, A. Jurjiu, and T. Koslowski, Macromolecules **37**, 638 (2004).

- [20] D. K. Wójcik and J. R. Dorfman, Phys. Rev. Lett. **90**, 230602 (2003).
- [21] K. Ito, ed., *Encyclopedic Dictionary of Mathematics* (MIT-Press, 1987).
- [22] E. Farhi and S. Gutmann, Ann. Phys. **213**, 182 (1992).
- [23] A. Wójcik, T. Łuczak, P. Kurzyński, A. Grudka, and M. Bednarska, Phys. Rev. Lett. **93**, 180601 (2004).